RESEARCH PAPER

Modified polystyrene−chitosan composite as an electrolyte membrane: Structure−property relationship

Kholoud A. Afifi [a], Mohamed A. Saied [b], Najwa A. Khaleq [a], Alaa Fahmy [c,a,*]

[a] Department of Chemistry, Faculty of Science (Girls), Al-Azhar University, Cairo, Egypt
[b] Department of Polymeric Materials Research, Advanced Technology and New Materials Research Institute (ATNMRI), The City of Scientific Research and Technological Applications (SRTA-City), Egypt
[c] Department of Petrochemicals, Faculty of Engineering, Pharos University, Alexandria, Egypt

Abstract

Modified polystyrene (PS)−chitosan (CS) composite membranes were prepared in depending on the ratios of CS to PS matrices, and structure−property relationship was discussed. Fourier transform infrared(, scanning electron microscope, and thermogravimetric analysis techniques were used to evaluate the chemical composition, surface topography, and thermal stability, respectively. In addition, investigations were conducted on mechanical strength, water and ethanol uptakes, ion exchange capacity as well as proton conductivity (PC). The sulfonation process was approved by Fourier transform infrared analysis, which revealed a characteristic absorption band at 1377−1300 and 3450 cm^{-1}. The thermogravimetric analysis reveals that the obtained membranes are thermally stable up to 300 °C. The ion exchange capacity values for sulfonated PS and sulfonated PS with 0.05% CS were 0.95 and 0.98 mEq/g, respectively, which were greater than those testified for Nafion 117 membranes (0.91 mEq/g). However, the sample containing 0.06% CS had the best mechanical properties. Importantly, there was a noticeable increase in PC ranging from 0.12 to 0.17 S/cm with the incorporation of 0.05% of CS. This accomplishment exceeds the documented PC value of 0.084 S/cm for Nafion 117.

Keywords: Chitosan, Composite, Electrolyte membrane, Fuel cells, Modified polystyrene

1. Introduction

The current global direction is focused on exploring and advancing renewable energy sources like solar power and fuel cells. To effectively compete for traditional fossil fuel options such as coal, natural gas, and gasoline, it is crucial to enhance the cost-effectiveness and reliability of renewable energy resources.[1,2] The continuous consumption of fossil fuels is rapidly depleting their reserves, posing challenges to meet future energy needs. Fuel cells, however, offer several significant advantages as a clean energy source. These include minimal noise pollution, reduced environmental contamination, and nearly zero emission of byproducts. Therefore, fuel cells are widely regarded as a promising clean energy resource.[2,3]

DuPont's Nafion, a perfluorinated ionomer, is composed of poly(tetrafluoroethylene) backbones with perfluoroetheral side chains terminated by sulfonic acid groups.[4] It has found widespread use in hydrogen and direct ethanol fuel cells (DEFC) due to its exceptional thermal, chemical, and mechanical stability, along with high proton conductivity (PC).[5,6] However, challenges such as susceptibility to degradation at high temperatures, low ionic conductivity under low humidity, elevated methanol permeability, and high production costs have hindered its application in these technologies.[7,8] Consequently, numerous academic and

Received 12 September 2023; revised 14 January 2024; accepted 28 January 2024.
Available online 8 April 2024

* Corresponding author at: Department of Chemistry, Faculty of Science (Girls), Al-Azhar University, Cairo, Egypt.
E-mail address: alaa.fahmy@azhar.edu.eg (A. Fahmy).

https://doi.org/10.62593/2090-2468.1013

industrial research groups have endeavored to develop polymer-based systems as potential alternatives to replace Nafion in proton exchange membranes (PEMs). Nafion is an extensively employed membrane as PEM. Nafion 115, Nafion 117, Nafion 111, and Nafion 112 are examples of nonreinforced films with varying thicknesses. The selection of the appropriate thickness is primarily based on its compatibility with the prepared blended membranes.[9] Numerous natural or artificial polymers were modified or grafted with sour groups, primarily sulfonic groups, through chemical processes. Besides, blending of polymers or creating polymer composites with inorganic nanoparticles has been explored.[10] However, a significant limitation of DEFC is the loss of ethanol across the PEM and the challenge of developing highly responsive PEM that can effectively manage water.[9] Furthermore, fouling is a concern that can adversely impact polymeric membranes, leading to a reduction in their efficiency by obstructing the proton-binding sites. This fouling can occur due to impurities in the fuel or as a result of biological and chemical interactions.[11] When a polymeric membrane becomes fouled, it either needs to undergo a recovery process or be replaced, thereby increasing the cost and decreasing the operational efficiency.[12] Among the synthetic polymers that have drawn considerable attention in developing polyelectrolyte membranes for DEFCs, polystyrene (PS) which is derived from styrofoam waste which is considered cost-effective. Nevertheless, the membrane exhibits very poor PC. Thus, the alternative method has become the focus of many researchers to treat these types of expanded waste, namely chemical recycling as well because of its low impact on the environment. Several papers have focused on converting of PS waste by sulfonation into a polyelectrolyte.[13,14]

This modification introduces sulfonate groups attached to the benzene ring.[15] The combination of sulfonated polystyrene (SPS) with either natural or synthetic polymers has been recognized as a viable approach in the literature, demonstrating the feasibility of developing polyelectrolyte membranes through such blending strategies. The incorporation of chitosan (CS) serves as a strategic selection as a membrane filler, primarily due to its cost-effectiveness, sourced from marine waste, and widespread availability. Furthermore, the presences −OH and NH_2 groups in CS contribute to its ionic nature, enhancing the overall membrane conductivity. SPS−CS composite materials were used for biological applications.[16] Gaur et al.[17] prepared a proton-conducting polymer electrolyte nanocomposite membrane using poly (vinyl alcohol) (PVA), CS, and poly (styrene sulfonic acid) (PSSA) polymers and montmorillonite CloisiteVR 30B clay with the objective of its application in direct methanol fuel cells. Methanol permeability of the PVA/PSSA/CS/Cloisite30B clay composite membrane has been found to be superior to that of PVA/PSSA as well as Nafion 117 membranes. The negative point is that the water uptake of the membrane is much higher than that of Nafion 117. Opier and Siswanta[15] studied the adsorption of Cd(II) ions and Pb(II) ions using CS−SPS. The adsorption experiment was performed under various conditions such as weight ratios of SPS and CS as adsorbent, pH, contact time, and different initial Cd(II) and Pb(II) concentrations. The optimum conditions were ratio: SPS: CS 60 : 40, pH value: 4 for Cd(II) ions and 5 for Pb(II) ions.

PS is a polymer extensively utilized in various fields, including protective packaging, food containers, electronics, and building materials. Its versatility makes it suitable for various industries and purposes.[18,19] Furthermore, PS comprises ~10% of global plastic production due to its affordability.[20] PS modified with sulfonic groups finds applications in diverse subjects, involving water treatments,[21] CO_2 arrest and separation, and fuel cells, owing to its superior conductivity,[22,23] sensors,[24] stimuli-responsive photonic crystals, ion exchange membranes,[25] and catalysts.[26] The resulting products of PS with a low degree of sulfonation might be utilized as membranes that can be used for fuel cell applications.[27]

Deacetylation of chitin is a good way to obtain CS, which is a carbohydrate polymer used in a wide range of applications. It has sound characteristics such as being renewable, harmless, and ecofriendly, and can be primarily sourced from the exoskeletons of shellfish and insects. CS is a copolymer composed of glucosamine and N-acetylglucosamine units joined by 1−4 glucosidic bonds. Due to its biodegradable nature, lack of toxicity, biocompatibility, and antifungal properties, CS and its derivatives were applied extensively in various fields such as tissue engineering, biological split systems, medication, and makeups.[28] However, creating an electrolyte membrane using pure CS for fuel cell applications is challenging due to its low PC, low thermal stability, and high water transport. Typically, a common approach to address this issue is to blend different polymers to obtain a new material with a diverse range of properties.[29,30] In conclusion, PS waste is problematic for the environment because of its chemical inertness, its low density which leads to the consumption of burial places, and the difficulty of biodegradation. Therefore, in this work an innovative material such as styrofoam

waste is chemically modified into a valuable material and blended with CS biopolymer. CS source is marine waste which in turn reduces the cost of membrane production and is widely available. According to our best knowledge, this composite membrane from SPS/CS is no prior instance of its preparation. Therefore, the main aim of this work is to modify PS waste and blend it with CS to form a membrane with certain water uptake, PC, and thermal stability and to evaluate it as a PEM.

2. Materials and methods

2.1. Materials

Waste foam was utilized as the source material to obtain PS. The foam is rinsed with a combination of water and methanol, then dried, and cut into small pieces. To dissolve the PS, a 10% (w/v) solution of PS was prepared using chloroform. Chloroform was obtained from Alpha Chemika, Maharashtra, India. H_2SO_4 (98%) is utilized as a sulfonating reagent (purchased from Acid Fischer, England, UK) and CS (MWT 10 000 g/mol > Mw ≤ 2500 g/mol) from Techno Pharmcem, Delhi, India. The Milli-Q EQ 7000 ultrapure water was used as a source of ultrahigh purified water (Millipore, resistivity >18 MΩ/cm).

2.2. Sulfonation of polystyrene

A measure of 5 g of styrofoam was dissolved in 30 ml chloroform. Next, a gradual dropwise addition of 3 ml of sulfuric acid (H_2SO_4, 98%) was carried out. The result was mixed for ~1 h at 50 °C to get the brown color. Subsequently, the suspended solution was filtrated, and the solid polymer was obtained, followed by thorough rinsing with distilled water to eliminate any excess of acids. Finally, the polymer was dried at 65 °C for 48 h.[19]

2.3. Preparation of sulfonated polystyrene-chitosan composite membranes

A solution of SPS (2.5 g) was prepared with a concentration of 10% wt in DMF (25 ml). CS with ratios of 0.05, 0.06, and 0.10% w/w was added to the prepared solution of SPS. By gradually adding CS slurry into the polymer solution, the mixture is gently stirred. The slow addition and continuous stirring prevent the agglomerates of CS. The mixing speed should be controlled to avoid excessive shear forces, which can lead to agglomeration. Also, ultrasonication was used to further disperse the CS particles. The high-frequency sound waves create microcavities and induce agitation in the solution, breaking down agglomerates and ensuring even dispersion. The composite mixture was subjected to ultrasonic sonication at 60 °C while stirring for 1 h. Afterward, the mixture is poured into a Petri dish and placed in an oven at 65 °C for 48 h to ensure complete drying as shown in Fig. 1. The membrane thickness was measured using a digital caliper.[15,16]

2.4. Characterizations and physical methods of measurements

The verification of the chemical composition of the prepared membranes was conducted using an Fourier transforms infrared spectroscopy (FT-IR). This analysis encompassed a wavenumber range scanning from 400 to 4000 cm^{-1}, while a high-resolution scanning electron microscopy (HRSEM) was used to investigate the morphological characteristics and microstructures of the polymeric materials and their membranes. The HRSEM analysis was performed using a Quanta FEG 250 instrument equipped with a field emission gun. Tensile testing was used to evaluate the mechanical properties of the blend, utilizing a universal testing machine, while

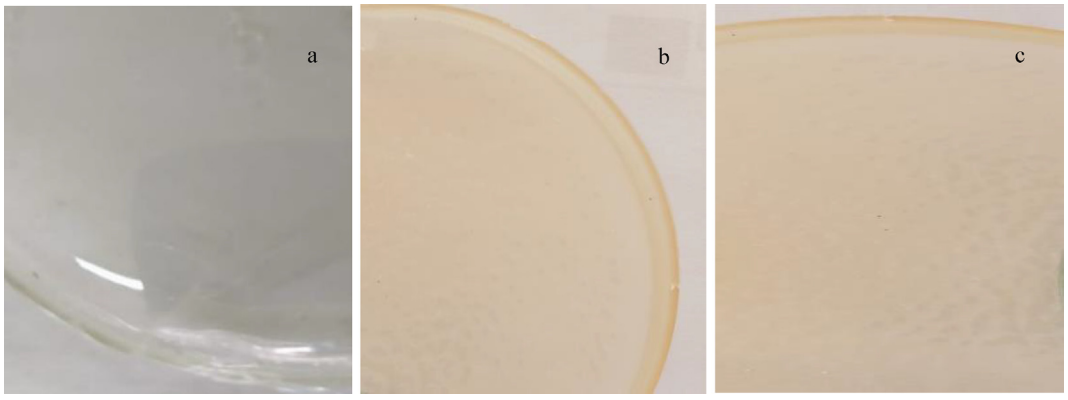

Fig. 1. Real image of (a) pure PS, (b) SPS, and (c) SPS/CS (0.05% of CS) membranes. CS, chitosan; PS, polystyrene; SPS, sulfonated polystyrene.

thermal properties of the prepared membranes were assessed using thermogravimetric analysis (TGA). The TGA analysis was conducted using a Shimadzu TGA-50 instrument, with the temperature range set from 30 to 800 °C and a heating rate of 10 °C/min. Ion exchange capacity (IEC) is a standard method to determine the quantity of free H^+ by submerging a specific volume of the membranes.[31] The IEC, represented as milliequivalents per gram of dry sample, is determined based on the recorded number of functional groups as shown in Eq. (1):

$$IEC = V\frac{N}{W_t} \tag{1}$$

where IEC is the ion exchange capacity, V the titrating value (ml), N the normality of NaCl, and W_t is the weight of dry polymer membrane (g). Also, the PC characteristics of composite membranes (SPS/CS) were evaluated using an AC impedance analysis performed with an AC impedance analyzer. Before the measurements, the sample membranes were immersed in a 2 M H_2SO_4 solution at room temperature.[28] Subsequently, films were positioned between two platinum electrodes that were designed to block ion movement. Impedance results derived from fitting Nyquist diagrams, which provide the relationship between the real (ϵ') and imaginary (ϵ'') components of permittivity for these samples were measured across a frequency range spanning from 100 kHz to 10 Hz.[32–34] These measurements were conducted under fluctuating voltage conditions (5 mV) and within a temperature interval of 25–80 °C, all under dry H_2 and O_2 atmospheres. The values for ionic conductivity were derived using the equation.[35]

$$\sigma = \frac{L}{RDW} \tag{2}$$

where σ is the PC (S/cm), L the distance between two electrodes (cm), and R the measured resistance for the samples(ohm), D the membrane thickness (cm), and W is the width of the membrane. The water and ethanol absorption of the prepared SPS–CS composite membranes was evaluated, and their performance was compared with pure SPS and pure CS membranes used as blanks. To assess the swelling efficiency of the prepared membranes, square-shaped samples with a length of 2 cm were cut and dried in a vacuum oven for 12 h. The initial weight of the dry samples was recorded as W_{dry}. Subsequently, at room temperature, the dried samples were submerged in deionized water and ethanol. At specific time intervals, such as 24 h, the samples were weighed again (W_{wet}) after being exposed to each solvent. The uptake of the solvents by the samples was calculated using Eq. (3) as follows:

$$Uptake(\%) = \frac{W_{wet} - W_{dry}}{W_{dry}} \times 100 \tag{3}$$

where W_{wet} is the weight of sample after soaking in solvent W_{dry} is the weight of sample before soaking.

3. Results and discussion

3.1. Fourier transform infrared

The FT-IR spectra of PS (Fig. 2a) exhibited distinct peaks. These peaks were identified as follows:

(a) peaks between 3050 and 3000 cm^{-1} represented the stretching vibrations of aromatic C–H bonds, (b) peaks in the vicinity of 1600–1580 cm^{-1} indicated the stretching vibrations of aromatic C=C bonds, (c) other peaks were observed at ~1500–1450 cm^{-1}, corresponding to C–H bending vibrations, and (d) at 1000–700 cm^{-1}, associated with C–H out-of-plane bending vibrations. Moreover, there were peaks in the range of 700–600 cm^{-1}, indicating aromatic C–H deformation vibrations.[36–38] The major peaks in the FT-IR spectra of SPS (Fig. 2b), corresponding to the chemical bonds present in pure PS membranes, as mentioned earlier, were observed, where chemical linkages in the range 3600–3200 cm^{-1} corresponds to the stretching of –OH in the $-SO_3H$ and NH groups[16] as reported by Jalal et al..[2] These peaks are attributed to the association with water molecules bonded to sulfonic acid by hydrogen bonds.

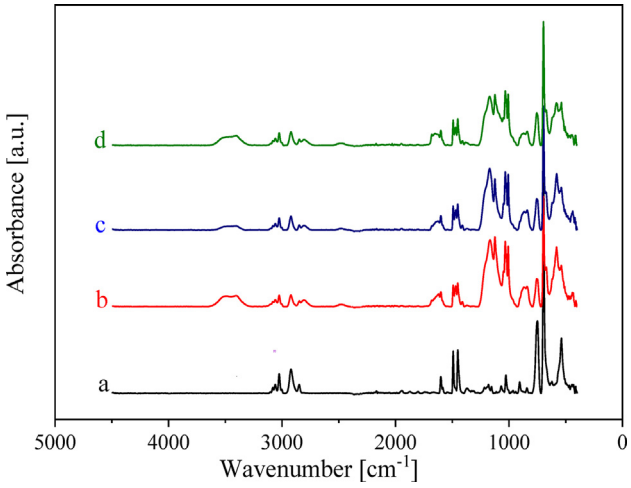

Fig. 2. FT-IR spectra of (a) pure PS, (b) pure SPS, and (c) SPS/CS composite membrane with different ratios of CS: 0.05, and (d) 0.10%. CS, chitosan; FT-IR, Fourier transform infrared; PS, polystyrene; SPS, sulfonated polystyrene.

The FT-IR spectra of SPS (Fig. 2b) clearly showed extra peaks, indicating the presence of sulfonic acid groups. These peaks were typically observed around 1200–1000 cm^{-1}, representing the stretching vibrations (S=O) of the sulfonic acid groups. In addition, peaks were observed around 3600–3000 cm^{-1}, indicating stretching vibrations (O–H) of sulfonic acid groups.[19,39]

Notably, with an increase in the concentration of sulfonic groups in the polymer chain, the absorption bands exhibit broadening, particularly in the 1200–1168 cm^{-1} range, corresponding to the asymmetric and symmetrical elongation of SO_2.[12] These observations provide evidence of the successful incorporation of sulfonated acid groups (-SO_3H) into the aromatic ring structure.[16,40]

The spectra of SPS and CS in the CS-SPS membrane were examined (Fig. 2c and d). A detected peak at 1451 cm^{-1} indicated the presence of the aromatic C=C vibration from the benzene ring in SPS. In addition, shifting vibrations of $-SO_3$ were noted at 1038 and 1061 cm^{-1} in the spectra.[41] At the wavenumber 1583 cm^{-1}, we observed and recorded overlapping vibrations of C–O and –NH.[42] Moreover, the presence of -C-S was confirmed by the absorption at 1126 cm^{-1}; in contrast, CS is a cationic polysaccharide comprising amine groups. CS's amine group presence provides a positive charge, facilitating the formation of ionic bonds with the negatively charged sulfonic groups in SPS. As a result, an ionic bond is formed between CS and SPS in the composite material (Scheme 1).[15] Consequently, the absence of the band at 1560 cm^{-1}, which is attributed to the $-NH_2$ groups, indicates the occurrence of ionic binding.[16,43,44]

3.2. Thermal stability

Only one weight loss stage was observed for pure PS at 400–440 °C, which was attributed to the main chain degradation (Fig. 3). The main chain degradation of SPS is lower than that observed in pure PS. The weight loss goes beyond 100 °C up to about 120 °C is due to the presence of water bound to SO_3H by H bonding in the thermogram of SPS. Another decomposition step is observed around 300 °C and continues to 350 °C, which is likely associated with the elimination of sulfonic acid groups or due to the loss of additives which is added during the extrusion and blowing agent used during the expansion step before the foaming process. During this stage, the reduction in weight loss could also be attributed to the volatilization of any remaining solvent. Even though the solvent's boiling point is notably lower than the temperature range associated with weight loss, it is crucial to consider the polymer's rubbery state. At the rubbery state, increase in free volume, along with the improved

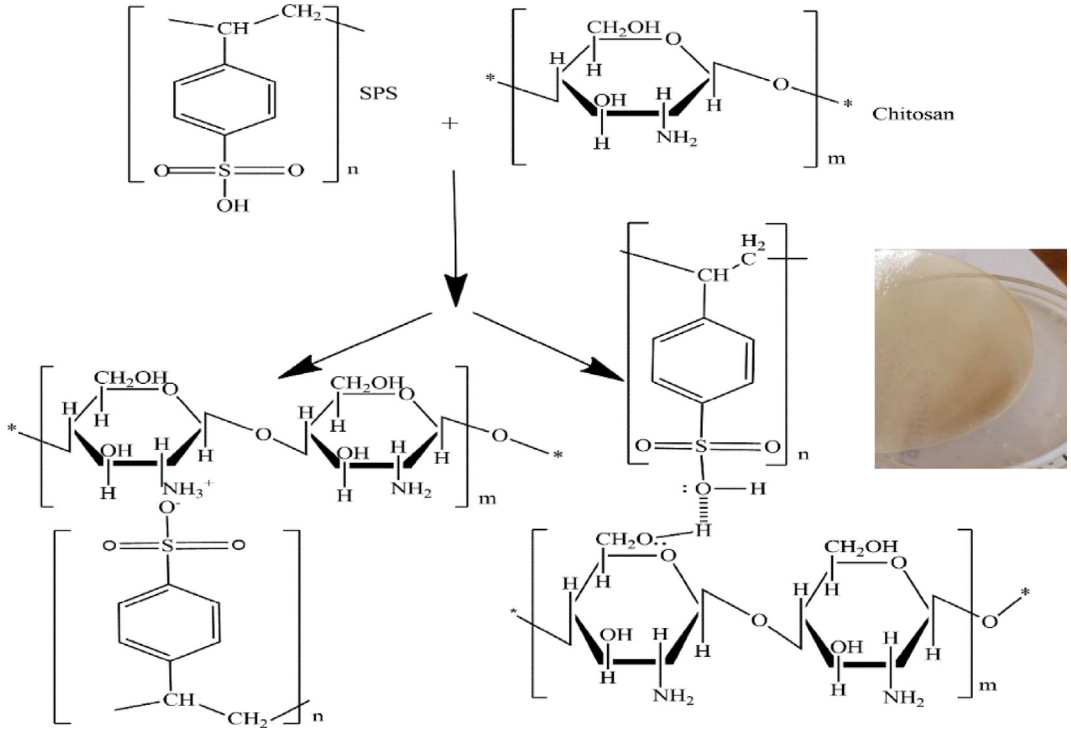

Scheme 1. Schematic diagram of supposing interaction of CS with SPS ionically and intermolecular hydrogen bonding. SPS, sulfonated polystyrene.

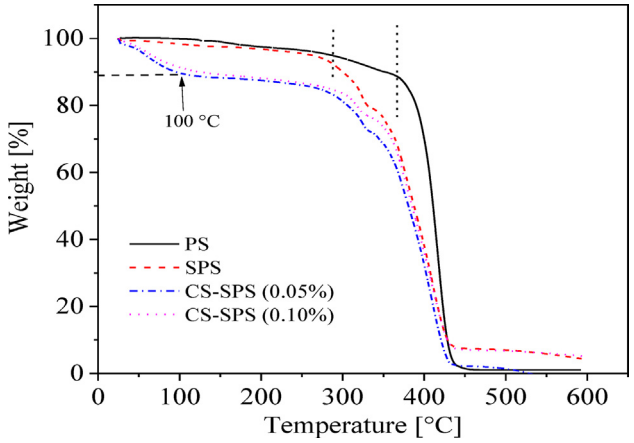

Fig. 3. TGA curves of pure PS, SPS blank, and CS-SPS composite with different ratio of CS: 0.05 and 0.10%. CS, chitosan; PS, polystyrene; SPS, sulfonated polystyrene; TGA, thermogravimetric analysis.

movement and sliding of polymer chains with increasing temperature, facilitates the evaporation of any trapped residual solvent within the polymer in its glassy state. Consequently, weight loss occurs at temperatures significantly higher than the boiling point of the solvent.[45,46]

The sulfonation process applied to CS–SPS composite membranes results in the formation of a highly acidic polyelectrolyte membrane. Consequently, these factors result in alterations in the membrane's decomposition behavior. The sulfonated membrane displays a three-step decomposition pattern, as evidenced by the presence of three distinct transitions in thermograms. The first step of decomposition occurs below 100 °C and extends up to ~110 °C. The reason for the weight loss can be traced back to the moisture evaporation within the membrane during the initial heating process, which suggests the development of a membrane possessing strong electrophilic properties. Around 300 °C, the second decomposition stage occurs. The weight loss during this step is linked to the removal of sulfonic acid groups from the membrane matrix. The final decomposition step takes place at 370 °C. This event is ascribed to the decomposition of the CS–SPS composite backbone.[47]

3.3. Water and ethanol uptakes

Water uptake is one of the main factors that refers to chemical stability, swilling, and cross-linking performance. Usually, low water uptakes possess high chemical stability and low degradation rate mainly in aqueous mediums. However, water uptake may provide a more direct estimation of methanol and water crossover, which is the one of important factors that must be considered in DMFC membrane.[48] The study of swelling ability is reported in Fig. 4a (uptake %) of the blank membrane compared with composite membranes. The swelling test performed at room temperature with deionized water and ethanol highlighted the potential appropriateness of the composite membrane for fuel cell utilization. The findings suggest that the composite membrane shows a positive reaction to these solvents, implying its potential effectiveness in fuel cell applications.[48]

The study demonstrated that with an increase in the ratio of CS polymer, the uptake of water and ethanol decreased. This observation can be explained by the water uptake of the modified SPS membrane, which exhibits a high ratio of 86.26% and an increase in the uptake value, which is caused by sulfonation process in order to unoccupied groups such as $-SO_3H$ groups, which can form hydrogen bond and hold more water molecules. The addition of 0.05% CS leads to the increase of water uptake dramatically. This behavior can be explained by the low combability between CS and membrane components leading to increase of the

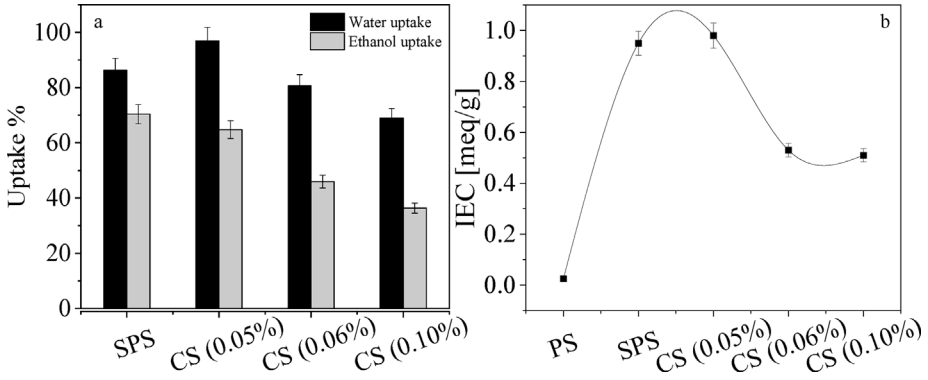

Fig. 4. Water and ethanol uptake (%) within 24 h (a) and IEC values (b) of pure PS, SPS, and CS-SPS composite with different ratios of CS: 0.05, 0.06, and 0.10%. CS, chitosan; IEC, ion exchange capacity; PS, polystyrene; SPS, sulfonated polystyrene.

water uptake to 97% low cross-linking density and holding more water. As well, the CS polymer has anionic characteristics that embed much water within the membrane structure due to an increase in the number of hydrophilic −OH, $-NH_2$ groups of CS along with the $-SO_3H$ groups of SPS. Increasing in molar ratio of CS (up to 0.10%) leads to obtain a membrane with low water uptake (68.96%). As a result of the intermolecular hydrogen bonding interaction between the polymers, particularly involving the terminal hydroxyl groups. Another factor that may play a role is the amine group present in CS, which imparts a positive charge and allows for ionic binding with the negatively charged sulfonate groups of SPS. As a result of this interaction, a polymer film with strong cross-linking is formed.

Second, upon incorporation of CS (0.05, 0.06, and 0.10%) blend to SPS membrane, the amount of ethanol taken possesses lower values of 64.56, 45.44, and 36.36%, respectively. This is a result of the size of ethanol molecules being larger than the size of water molecules. Hence, its movement can be obstructed by the CS polymer chain. Also, the blocking effect occurs due to the interaction of the terminal function group for both blended polymers. As the amount of CS grew to 0.10% w/v the amount of ethanol taken progressively decreased and reached 36.36%. The ability of SPS and CS to form a strong cross-linking film increases.[49]

3.4. Ion exchange capacity

The IEC value serves as an indirect estimation of PC. Fig. 4b presents a comparison of the IEC values between CS−SPS composite membranes, pure PS, and SPS. As expected, the IEC value of the PS membrane is remarkably low, indicating a limited number of charges within the polymer membrane. Conversely, the IEC value of SPS is significantly higher than that of PS, primarily due to the presence of conducting groups ($-SOH_3$), which play a crucial role in enhancing the membrane's conductivity.

Moreover, the IEC for CS−SPS composite membrane was discussed based on the ratio of CS in the membrane. It was found that the highest value of IEC was recorded for the lowest amount (0.05%) of CS in the membrane and it is even higher than Nafion.[50] The IEC values exhibit a clear increase from 0.95 mEq/g for SPS to 0.98 mEq/g for 0.05% CS. Notably, this value surpasses the IEC reported for Nafion 117 in previous literature, which was 0.91 mEq/g.[51] This increase is due to the presence of ionic groups originating from the −OH and $-NH_2$ functional groups found in constituents within the structural framework of CS. This, in turn, results in an increase in the number of conductive groups, consequently enhancing conductivity levels. However, high percentages of CS give undesirable results, and this is expected from the interaction between the polymer chains forming intermolecular hydrogen bonds that led to blocking conductive group, which has the main effect to enhance the IEC value. Importantly, there was a noticeable increase in PC ranging from 0.12 to 0.17 S/cm when incorporating 0.05% of CS. This accomplishment exceeds the documented PC value of 0.084 S/cm for Nafion 117.

3.5. Proton conductivity

Investigating FC membrane performance, particularly regarding PC, holds paramount importance (Fig. 5a). In its pristine state, the PS membrane exhibited a PC value of 0.001 S/cm due to a limited count of ionic groups. Upon sulfonation of PS, the introduction of additional sulfonic groups led to a remarkable increase in PC, elevating it from 0.001 to

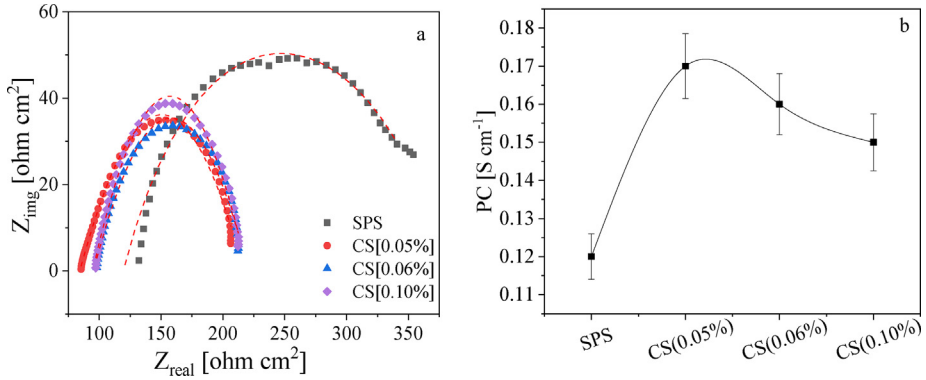

Fig. 5. Nyquist diagrams (a) and the PC values (b) of SPS, and CS-SPS composite with ratios of 0.05, 0.06, and 0.10% of CS. CS, chitosan; PC, proton conductivity; SPS, sulfonated polystyrene.

0.12 S/cm as shown in Fig. 5b. This enhancement can be attributed to the emergence of $-SO_3$-H^+ groups resulting from the sulfonation process, serving as an effective proton carrier.[34] Notably, the observed rise in PC extended from 0.12 to 0.17 S/cm for CS with a 0.05% ratio as presented in Table 1 and Fig. 5b. This achievement surpasses the documented value for Nafion 117, which stands at 0.084 S/cm.[28]

The enhancement owes itself to the presence of −OH and $-NH_2$ groups within the CS polymer. These molecular components play a pivotal role in augmenting PC and strengthening the polymer's anionic characteristics. However, as the proportion of CS in the membrane increases, a counterproductive effect becomes evident: the PC value experiences a noticeable reduction. This phenomenon stems from interactions between polymer chains, leading to the formation of intermolecular hydrogen bonds. Consequently, the count of ionic groups diminishes, which plays a critical role in elevating PC levels, as illustrated in Fig. 5.

Furthermore, it is important to note that the PC results for the CS ratio of 0.10% exhibit a significant deviation. These findings surpass the outcomes obtained from pure SPS alone. This disparity can be attributed to the nature of PC, which measures the degree of proton mobility between distinct groups along polymer chains, subsequently influencing electrical conductivity. However, the presence of linkages among these groups can impede the unrestricted motion of protons within the SPS structure. This obstruction becomes more noticeable due to the uneven distribution of these interconnections in a specific manner along the polymer chain, further hampering smooth movement. Consequently, the efficiency of free proton mobility diminishes, resulting in a decrease in the recorded value. Fig. 5 provides a visual representation of the relationship between the real part of impedance (Z_{real}) and the imaginary part of impedance (Z_{img}) across different concentrations of PEMs. This includes composite membranes of SPS–CS at concentrations of 0.05, 0.06, and 0.10% CS, alongside pure SPS. These instances shed light on how distinct frequencies influence impedance patterns. Through careful analysis of the Nyquist diagram, we extracted resistance values. These values were subsequently harnessed in the calculation of PC, as outlined in the preceding equation (Eq. 2).

3.6. Surface morphology

HRSEM was used to examine the surface morphology of the CS–SPS composite membrane at different CS ratios, with pure PS and SPS used as reference samples. Fig. 6a shows the morphology of pure PS film and displayed a homogeneous and smooth surface with matrix tearing without any noticeable pores or cracks. The morphology of the SPS film exhibits a combination of hydrophobic and hydrophilic regions.

Hydrophobic regions are composed of the PS backbone, which is a nonpolar polymer. These regions are relatively impermeable to water and other polar solvents. The hydrophilic regions, on the contrary, in SPS membranes are composed of sulfonic acid groups that have been introduced into the PS backbone. As a result, the SPS membranes exhibit two distinguishable phases (Fig. 6b). However, these sulfonic groups are highly polar and attract water molecules, making them more permeable to water and other polar solvents. Thus, the morphology of SPS film can be further modified by varying the degree of hydrophilicity. Increasing the ratio of CS in the composite (Fig. 6c and d) increases the quantity of hydrophilic groups within the polymer. However, simultaneously, it enhances the interaction between the polymer chains, resulting in the formation of intermolecular hydrogen bonds that led to a reduction in its permeability to water and other polar solvents forming a cross-linked polymer as the obtained results from the TGA, uptake, and IEC. In general, the morphology of the SPS film is determined by a careful equilibrium between hydrophobic and hydrophilic regions, which can be adjusted by controlling the degree of electrophilicity.

3.7. Mechanical properties

Table 2 presents a summary of the mechanical properties observed in all the membranes analyzed

Table 1. Explanation of the resistance obtained from fitting of Nyquist diagrams and other factors for derived proton conductivity.

Samples	Resistances (Ohm)	Distances between electrodes (cm)	Thickness (cm)	Widths (cm)	Proton conductivity (S/cm)
SPS	187.4	1	0.40	10.87	0.12
CS (0.05%)	130.2	1	0.43	10.43	0.171
CS (0.06%)	121.6	1	0.46	11.16	0.160
CS (0.10%)	141.1	1	0.39	12.10	0.150

CS, chitosan; SPS, sulfonated polystyrene.

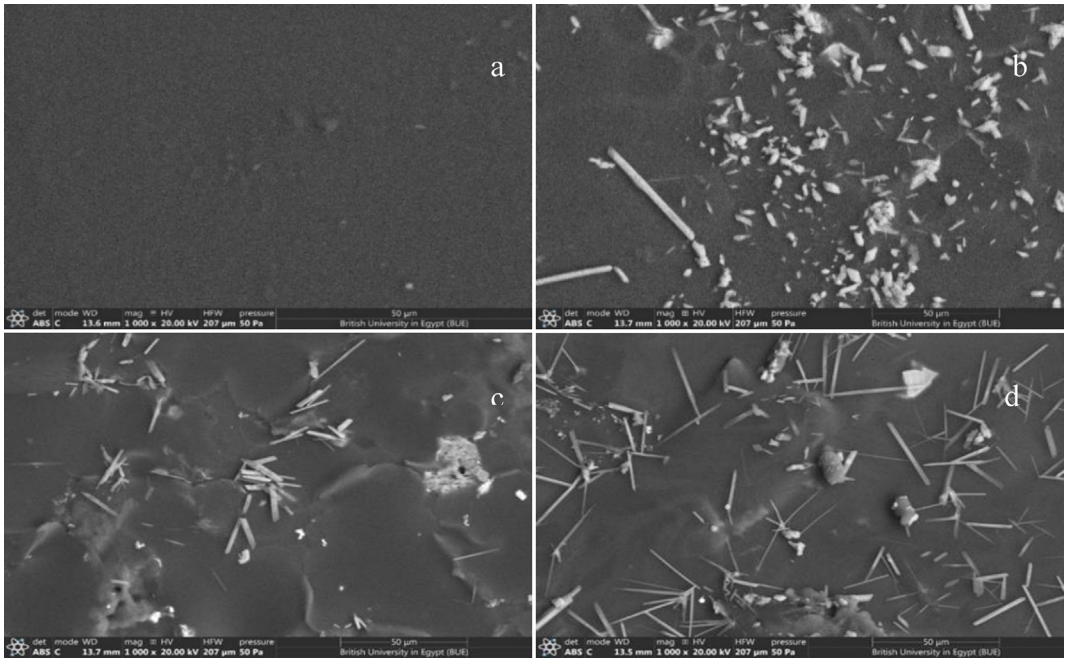

Fig. 6. SEM micrographs of (a) PS, (b) PSA, and CS–SPS composite membrane (c) (0.05% CS), and (d) (0.10% CS). CS, chitosan; SEM, scanning electron microscope; SPS, sulfonated polystyrene.

Table 2. The tensile strength of PSA/chitosan at various ratios of chitosan within the composite.

Materials	Maximum force (N/mm^2)	Maximum dispersion (mm)	Maximum stress (MPa)	Maximum strain (%)
Pure PS	40.469	0.281	80.938	00.935
SPS	03.750	1.621	07.500	05.403
CS (0.05%)	06.250	2.830	12.500	09.433
CS (0.06%)	45.469	3.051	27.656	06.658
CS (0.10%)	05.781	0.751	11.563	02.503

CS, chitosan; SPS, sulfonated polystyrene.

during the study. Considerable differences were noted in the strength of the membranes. By comparing the strength values among pure PS, SPS, and composite membranes with varying concentrations of CS%, the differences become evident indicating that the mechanical strength is influenced by the ratios of CS in the matrix. The mechanical strength of SPS–CS formulations with a 0.10% CS concentration was found to be lower compared with that of pure PS. This decrease in mechanical properties suggests that the addition of CS did not reinforce the sample, behaving as a nonreinforcing component. This decrease in strength can be attributed to the limited interfacial interaction between the various components of the blended membrane. This leads to a decrease in mechanical strength at the interface of the blends. Also, the reason may be some materials exhibit different strength properties in different directions due to their crystal structure or fiber alignment. If loads are applied in a direction of lower strength, the material might fail at lower stress levels. While the maximum stress of CS 0.05% ratio shows an increase in maximum stress than pure SPS, the reason is a balance between the free ionic groups that increase elastic properties and the number of ionic group that are interlinked, causing an increase in maximum stress. Moreover, Table 2 displays the shear strength values, encompassing the maximum force, dispersion, stress, and strain measurements.

Notably, the sample containing 0.06% CS exhibited the highest stress and only 6% strain. This indicates that this particular sample possesses the characteristics of a plastic material.[52] It may refer to the most ionic groups that can provide elastic characteristics for the membrane, which are blocked by intermolecular hydrogen bonds that provide the membrane with plastic features.

Tables 3 and 4 offer a brief overview of the state and different factors, including thickness, tensile

Table 3. Thickness, tensile strength, elongation at break, contact angle, ion exchange capacity, proton conductivity, and cost of sulfonated polystyrene–chitosan membranes compared with Nafon 117.

Membranes	Thickness (mm)	TS (MPa)	Elongation (%)	IEC (mEq/g)	PC (S/cm)	Cost 10 × 10 cm
SPS	0.40	7.50	5.40	0.95	0.122	~2.63 $
SPS–CS (0.05%)	0.43	12.500	09.433	0.98	0.171	
SPS–CS (0.06%)	0.46	27.656	06.658	0.63	0.160	
SPS–CS (0.10%)	0.39	11.563	02.503	0.62	0.150	
Nafion 117[53,54]	0.185	18.20	12.20	0.91	0.082	33 $
Nafion 112[55–57]	50.00	31.11	300.00	0.90	2.000	

IEC, ion exchange capacity; PC, proton conductivity; SPS, sulfonated polystyrene.

Table 4. Water uptake, ion exchange capacity, proton conductivity, and thermal stability of sulfonated polystyrene–chitosan membranes compared with other membranes.

Membranes	Water uptake (%)	IEC (mEq/g)	Proton conductivity (S/cm)	Thermal stability (°C)
SPS	84.26	0.98	0.122	Stable up to 300 °C
SPS–CS (0.05%)	97	0.63	0.171	
SPS–CS (0.06%)	80.64	0.62	0.160	
SPS–CS (0.10%)	68.96	0.67	0.150	
PVA/SPSA/chitosan/Cloisite30B[17]	258.00	1.03	0.0332	Stable up to 120 °C

IEC, ion exchange capacity; PVA, poly (vinyl alcohol); SPS, sulfonated polystyrene.

strength, elongation, contact angle, IEC, PC, cost, water uptake percentage, and thermal stability for SPS–CS membranes compared with Nafion-based membranes. The findings suggest that the SPS–CS membrane demonstrates potential as an electrolyte membrane.

3.8. Conclusions

The work presents an experimental study to prepare a composite ion exchange membrane composed of SPS and CS. The research involved a multistep process that started with sulfonation of styrofoam, followed by the conversion of discarded material into films using a casting technique. The sulfonation process was used to modify styrofoam waste and introduce sulfonic groups. The modified PS was then blended with CS to create SPS–CS composite membrane with varying ratios of CS (0.05, 0.06, and 0.10% CS). Subsequently, various characterizations were conducted, encompassing physical, chemical, thermal stability, and electrochemical properties, including IEC and ionic conductivity assessments.

The results indicate that the sulfonation process effectively modified PS by introducing sulfonic groups. These findings are supported by the results from FTIR analysis, IEC measurements, and solvent uptake studies. The SEM images of the SPS membrane showed the existence of both hydrophobic and hydrophilic regions. The mechanical properties of samples containing CS (0.06%) are much better than other samples. Its maximum stress is 27 MPa where strain is only 6%. All samples are considered thermally stable until 300 °C. The existence of −OH and $-NH_2$ functional groups within the CS polymer leads to an increase in PC, resulting in a range from 0.12 to 0.17 S/cm for CS with a ratio of 0.05%. This accomplishment exceeds the recorded value of 0.084 S/cm for Nafion 117.

Author contributions

Conceptualization: Alaa Fahmy and Mohamed Abu Saied; Methodology: Kholoud A. Afifi and Najwa Abdel Khaleq; Investigation: Kholoud A. Afifi and Mohamed Abu Saied; Writing—original draft preparation: Kholoud A. Afifi and Alaa Fahmy; Writing-review and editing: Alaa Fahmy.

Conflict of interest

There are no conflicts of interest.

Acknowledgment

This paper is based on work supported by the Science, Technology, and Innovation Funding Authority (STDF) under grant number 45109.

References

1. Li X, Zhang H, Mai Z, Zhang H, Vankelecom I. Ion exchange membranes for vanadium redox flow battery (VRB) applications. *Energy Environ Sci*. 2011;4:1147–1160.
2. Jalal NM, Jabur AR, Hamza MS, Allami S. Sulfonated electrospun polystyrene as cation exchange membranes for fuel cells. *Energy Rep*. 2020;6:287–298.
3. Khazaee I, Ghazikhani M. Performance improvement of proton exchange membrane fuel cell by using annular shaped geometry. *J Power Sources*. 2011;196:2661–2668.

4. Sun C, Zlotorowicz A, Nawn G, et al. [Nafion/(WO3)x] hybrid membranes for vanadium redox flow batteries. *Solid State Ionics*. 2018;319:110−116.
5. Winter M, Brodd RJ. What are batteries, fuel cells, and supercapacitors? *Chem Rev*. 2004;104:4245−4269.
6. Yang L, Zeng X, Wang W, Cao D. Recent progress in MOF-derived, heteroatom-doped porous carbons as highly efficient electrocatalysts for oxygen reduction reaction in fuel cells. *Adv Funct Mater*. 2018;28:1−21.
7. Hickner MA, Ghassemi H, Kim YS, Einsla BR, McGrath JE. Alternative polymer systems for proton exchange membranes (PEMs). *Chem Rev*. 2004;104:4587−4611.
8. Sangeetha D. Conductivity and solvent uptake of proton exchange membrane based on polystyrene(ethylene-butylene) polystyrene triblock polymer. *Eur Polym J*. 2005;41:2644−2652.
9. Xu J, Sheng GP, Luo HW, Li WW, Wang LF, Yu HQ. Fouling of proton exchange membrane (PEM) deteriorates the performance of microbial fuel cell. *Water Res*. 2012;46:1817−1824.
10. Abu-Saied MA, Soliman EA, Abualnaj KM, El Desouky E. Highly conductive polyelectrolyte membranes poly(Vinyl alcohol)/poly(2-acrylamido-2-methyl propane sulfonic acid) (PVA/PAMPS) for fuel cell application. *Polymers*. 2021;13:2638.
11. Rana D, Kim Y, Matsuura T, Arafat HA. Development of antifouling thin-film-composite membranes for seawater desalination. *J Membr Sci*. 2011;367:110−118.
12. Mahmoud A, Fahmy A, Naser A, Saied MA. Novel sulfonated poly (vinyl alcohol)/carboxy methyl cellulose/acrylamide-based hybrid polyelectrolyte membranes. *Sci Rep*. 2022;13: 2638.
13. Inagaki Y, Kuromiya M, Noguchi T, Watanabe H. Reclamation of waste polystyrene by sulfonation. *Langmuir*. 1999;15: 4171−4175.
14. Bajdur W, Pajczkowska J, Makarucha B, Sulkowska A, Sulkowski WW. Effective polyelectrolytes synthesised from expanded polystyrene wastes. *Eur Polym J*. 2002;38:299−304.
15. Opier RDA, Siswanta D. Synthesis of polyelectrolyte complex (PEC) membrane chitosan-polystyrene sulfonate (PSS) from styrofoam waste as adsorbents of Cd(II) and Pb(II) ions. *IOP Conf Ser Earth Environ Sci*. 2020;483:012028.
16. Eskandarloo H, Godec M, Arshadi M, Padilla-Zakour OI, Abbaspourrad A. Multi-porous quaternized chitosan/polystyrene microbeads for scalable, efficient heparin recovery. *Chem Eng J*. 2018;348:399−408.
17. Gaur SS, Dhar P, Kumar A, Katiyar V. Prospects of poly (vinyl alcohol)/Chitosan/poly (styrene sulfonic acid) and montmorillonite Cloisite®30B clay composite membrane for direct methanol fuel cells. *J Renew Sustain Energy*. 2014;6:053135.
18. Zhou J, Ritter H. Cyclodextrin functionalized polymers as drug delivery systems. *Polym Chem*. 2010;1:1552−1559.
19. Dardeer HM, Toghan A. A novel route for the synthesis of pseudopolyrotaxane containing γ-Cyclodextrin based on environmental waste recycling. *J Mol Struct*. 2021;1227:129707.
20. Xiaoting Fu TT, Ding M, Tang C, et al. Toughening of recycled polystyrene used for TV backset. *Appl Polym*. 2008;109: 3725−3732.
21. Siyal AN, Memon SQ, Parveen S, Khuhawar MY, Soomro A, Khaskheli MI. Chemical recycling of expanded polystyrene waste: synthesis of novel functional polystyrene-hydrazone surface for phenol removal. *J Chem*. 2013;8, 2013.
22. Fu Z, Jia J, Li J, Liu C. Transforming waste expanded polystyrene foam into hyper-crosslinked polymers for carbon dioxide capture and separation. *Chem Eng J*. 2017;323:557−564.
23. Fahmy A, Kolmangadi MA, Schönhals A, Friedrich J. Structure of plasma − deposited copolymer films prepared from acrylic acid and styrene : Part III sulfonation and electrochemical properties. *Plasma Process Polym*. 2022;19:2100222.
24. Nucara L, Piazza V, Greco F, et al. Ionic strength responsive sulfonated polystyrene opals. *ACS Appl Mater Interfaces*. 2017; 9:4818−4827.
25. Yi M, Hong S, Kim JR, et al. Modification of a PEDOT:PSS hole transport layer for printed polymer solar cells. *Sol Energy Mater Sol Cells*. 2016;153:117−123.
26. Ordomsky VV, Schouten JC, van der Schaaf J, Nijhuis TA. Foam supported sulfonated polystyrene as a new acidic material for catalytic reactions. *Chem Eng J*. 2012;207−208: 218−225.
27. Sulkowski WW, Nowak K, Sulkowska A, et al. Study of the sulfonation of expanded polystyrene waste and of properties of the products obtained. *Pure Appl Chem*. 2009;81:2417−2424.
28. Cui Z, Xing W, Liu C, Liao J, Zhang H. Chitosan/heteropolyacid composite membranes for direct methanol fuel cell. *J Power Sources*. 2009;188:24−29.
29. Kweon DK, Song SB, Park YY. Preparation of water-soluble chitosan/heparin complex and its application as wound healing accelerator. *Biomaterials*. 2003;24:1595−1601.
30. Karua CS, Sahoo A. Synthesis and characterization of starch/chitosan composites. *Mater Today Proc*. 2020;33:5179−5183.
31. Fahmy. A, Abu Saied MA, Morgan. N, et al. Modified polyvinyl chloride membrane grafted with an ultra-thin polystyrene film: structure and electrochemical properties. *J Mater Res Technol*. 2021;12:2273−2284.
32. Ma J, Choudhury NA, Sahai Y, Buchheit RG. A high performance direct borohydride fuel cell employing cross-linked chitosan membrane. *J Power Sources*. 2011;196:8257−8264.
33. Haragirimana A, Ingabire PB, Zhu Y, et al. Four-polymer blend proton exchange membranes derived from sulfonated poly(aryl ether sulfone)s with various sulfonation degrees for application in fuel cells. *J Membr Sci*. 2019;583:209−219.
34. Khalaf M, Saeed AM, Ali AI, Kamoun EA, Fahmy A. Polyelectrolyte membranes based on phosphorylated − PVA/cellulose acetate for direct methanol fuel cell applications : synthesis, instrumental characterization, and performance testing. *Sci Rep*. 2023;13:13011.
35. Ru C, Gu Y, Na H, Li H, Zhao C. Preparation of a cross-linked sulfonated poly(arylene ether ketone) proton exchange membrane with enhanced proton conductivity and methanol resistance by introducing an ionic liquid-impregnated metal organic framework. *ACS Appl Mater Interfaces*. 2019;11: 31899−31908.
36. Bekri-Abbes I, Bayoudh S, Baklouti M, Papon E, LeClercq D. Converting waste polystyrene into adsorbent: optimisation of reaction parameters and properties. *Prog Rubber Plast Recycl Technol*. 2006;22:179−193.
37. Fahmy A, Friedrich J. Degradation behavior of thin polystyrene fi lms on exposure to Ar plasma and its emitted radiation. *J Adhes Sci Technol*. 2013;27:324−338.
38. De León-Condés CA, Roa-Morales G, Martínez-Barrera G, et al. Sulfonated and gamma-irradiated waste expanded polystyrene with iron oxide nanoparticles, for removal of indigo carmine dye in textile wastewater. *Heliyon*. 2019;5:e02071.
39. Chipara DM, Macossay J, Ybarra AVR, Chipara AC, Eubanks TM. Applied surface science Raman spectroscopy of polystyrene nanofibers — multiwalled carbon nanotubes composites. *Appl Surf Sci*. 2013;275:23−27.
40. Francisco-Vieira L, Benavides R, Cuara-Diaz E, Morales-Acosta D. Styrene-co-butyl acrylate copolymers with potential application as membranes in PEM fuel cell. *Int J Hydrogen Energy*. 2019;44:12492−12499.
41. Mahmoud ME, Abdou AEH, Ahmed SB. Conversion of waste styrofoam into engineered adsorbents for efficient removal of cadmium, lead and mercury from water. *ACS Sustainable Chem Eng*. 2016;4:819−827.
42. Mahmoud A, Saied MA, Naser A, Fahmy A. Synthesis and characterization of nylon 6 , 6-polyvinyl alcohol-based polyelectrolytic membrane. *Arabian J Sci Eng*. 2022;48:8941−8956.
43. Sik D, Guiver MD, Yong S, et al. Preparation of ion exchange membranes for fuel cell based on crosslinked poly (vinyl alcohol) with poly (styrene sulfonic acid-co-maleic acid). *Ionics*. 2006;281:156−162.
44. Kamoun EA, Youssef ME, Abu-Saied MA, Fahmy A, Khalil HF, Abdelhai F. Ion conducting nanocomposite membranes based on PVA-HA-HAP for fuel cell application: II. Effect of modifier agent of PVA on membrane properties. *Int J Electrochem Sci*. 2015;10:6627−6644.

45. Biswas M, Chatterjee S. Chemical modification of polystyrene—IV. Electrophilic substitution of polystyrene with cis-1, 2, 3, 6 tetrahydrophthalic anhydride. *Eur Polym J*. 1983; 19:317−320.
46. Smitha B, Sridhar S, Khan AA. Synthesis and characterization of proton conducting polymer membranes for fuel cells. *J Membr Sci*. 2003;225:63−76.
47. Zubir NA, Ismail AF, Nasef MME, Haji K, Dahlan M, Saidi H. *Sulfonated polystyrene pore-filled electrolytes membranes by electrons induced grafting of styrene into PVDF films : thermal stability and structural investigation*. The 4th Annual Seminar of National Science Fellowship; 2004:568−573.
48. Abu-Saied M, Fahmy A, Morgan N, Qutop W, Abdelbary H, Friedrich JF. Enhancement of poly(vinyl chloride) electrolyte membrane by its exposure to an atmospheric dielectric barrier discharge followed by grafting with polyacrylic acid. *Plasma Chem Plasma Process*. 2019;39:1499−1517.
49. Dutta K, Das S, Kundu PP. Effect of the presence of partially sulfonated polyaniline on the proton and methanol transport behavior of partially sulfonated PVdF membrane. *Polym J*. 2016;48:301−309.
50. Wang L, Kang J, Nam J, Suhr J, Prasad AK. Composite membrane based on graphene oxide sheets and nafion for polymer electrolyte membrane fuel cells. *ECS Electrochem Lett*. 2015;4:1.
51. Abu-Saied MA, El-Desouky EA, Soliman EA, El-Naim GA. Novel sulphonated poly (vinyl chloride)/poly (2-acrylamido-2-methylpropane sulphonic acid) blends-based polyelectrolyte membranes for direct methanol fuel cells. *Polym Test*. 2020;89:106604.
52. Fahmy A, Mohamed TA, Abu-Saied M, Helaly H, El-Dossoki F. Structure/property relationship of polyvinyl alcohol/dimethoxydimethylsilane composite membrane: experimental and theoretical studies. *Spectrochim Acta Part A Mol Biomol Spectrosc*. 2020;228:117810.
53. Li C, Yang Z, Liu X, et al. Enhanced performance of sulfonated poly (ether ether ketone) membranes by blending fully aromatic polyamide for practical application in direct methanol fuel cells (DMFCs). *Int J Hydrogen Energy*. 2017;42:28567−28577.
54. Elerian AF, Abu-Saied MA, Abd-Elnaim GH, Elnaggar EM. Development of polymer electrolyte membrane based on poly(Vinyl Chloride)/graphene oxide modified with zirconium phosphate for fuel cell applications. *J Polym Res*. 2023;30:6.
55. Lin HL, Wang SH. Nafion/poly(vinyl alcohol) nano-fiber composite and Nafion/poly(vinyl alcohol) blend membranes for direct methanol fuel cells. *J Membr Sci*. 2014;452:253−262.
56. Kim SM, Ahn CY, Cho YH, et al. High-performance fuel cell with stretched catalyst-coated membrane: one-step formation of cracked electrode. *Sci Rep*. 2016;6:1−7.
57. Lee KH, Chu JY, Kim AR, Yoo DJ. Facile fabrication and characterization of improved proton conducting sulfonated poly(Arylene Biphenylether Sulfone) blocks containing fluorinated hydrophobic units for proton exchange membrane fuel cell applications. *Polymers*. 2018;10:1367.